UC San Diego
UC San Diego Previously Published Works

Title
Pore water pressure prediction for undrained heating of soils

Permalink
https://escholarship.org/uc/item/4sw2z1jr

Journal
Environmental Geotechnics, 4(2)

ISSN
2051-803X

Authors
Ghaaowd, Ismaail
Takai, Atsushi
Katsumi, Takeshi
et al.

Publication Date
2017-04-01

DOI
10.1680/jenge.15.00041

Peer reviewed

Pore Water Pressure Prediction for Undrained Heating of Soils

Ismaail GHAAOWD, M.S.[a], Atsushi TAKAI, Ph.D.[b], Takeshi KATSUMI, Ph.D.[c],
and John S. MCCARTNEY, Ph.D., P.E.[d, 1]

[a] *Doctoral Candidate, University of California, San Diego, Department of Structural Engineering, 9500 Gilman Dr. La Jolla, CA 92093-0085,USA, ighaaowd@eng.ucsd.edu.*
[b] *Assistant Professor, Kyoto University, Graduate School of Global Environmental Studies, Yoshida-honmachi, Sakyo, Kyoto 6068501, Japan, takai.atsushi.2s@kyoto-u.ac.jp.*
[c] *Professor, Kyoto University, Graduate School of Global Environmental Studies, Yoshida-honmachi, Sakyo, Kyoto 6068501, Japan, katsumi.takeshi.6v@kyoto-u.ac.jp.*
[d] *Associate Professor, University of California, San Diego, Department of Structural Engineering, 9500 Gilman Dr. La Jolla, CA 92093-0085,USA, mccartney@ucsd.edu.*

Abstract

This paper focuses on the validation of a prediction model for the thermally induced excess pore water pressure generated in saturated soils during undrained heating. A thermo-elastic analysis was calibrated using experimental data presented in the literature for normally consolidated soils having different mineralogical compositions. The magnitude of thermally induced excess pore water pressure for these soils was observed to depend on the initial void ratio, the initial effective stress, the thermal coefficient of cubical expansion of the soil particles, the change in temperature, the compressibility of the soil skeleton, and the physico-chemical coefficient of structural volume change. An empirical relationship between the physico-chemical coefficient of structural volume change and the plasticity index was proposed to predict the thermally induced excess pore water pressure for saturated, normally consolidated soils. To validate the model, an undrained heating test was performed independently on a specimen of normally consolidated kaolinite clay, and the measured thermally induced excess pore water pressures were found to match well with the model predictions.

Keywords. Pore water pressure; thermal volume change; clay; geomaterial characterization; testing and evaluation.

List of notation

α_w is the cubical coefficient of thermal expansion of the pore water

α_s is the cubical coefficient of thermal expansion of the mineral solids

V_w is the initial volume of pore water before heating is the volume of solids

V_s is the volume of solids

---

[1] Corresponding author.

36	V_m	is the total volume of the soil mass equal to the sum of V_w and V_s
37	ΔT	is the change in temperature of the soil
38	ΔV_{st}	is the volume change of the soil due to the reorientation and relative movement of the soil
39		particles during heating
40	m_v	is the compressibility of the soil skeleton
41	m_w	is the compressibility of the water
42	n	is the porosity of a saturated soil
43	α_{st}	is the physico-chemical coefficient of structural volume change
44	$(m_v)_r$	is the compressibility of the soil skeleton determined from the recompression curves
45	e_0	is the initial void ratio
46	p'	is the mean effective stress
47	p'_c	is the mean effective preconsolidation stress
48	e_0	is the initial void ratio
49	σ'	is the effective stress
50	w	is the water content
51	LL	is the liquid limit
52	PL	is the plastic limit
53	LI	is the liquidity index
54	PI	is the plasticity index
55	κ	is the slope of the recompression line
56	λ	is the slope of the compression line
57	v	is the specific volume

1. Introduction

It is well known that undrained heating of saturated clays leads to excess pore water pressure generation due to the differential expansion of the pore water and soil solids (Campanella and Mitchell 1968). This phenomena also occurs in other saturated geomaterials, and is also referred to as thermal pressurization (Ghabezloo and Sulem 2009). As a measure for preconsolidation of soft clay layers, combining thermal energy from embedded geothermal heat exchangers with vertical drains to cause thermal consolidation can be effective in preparing a site for subsequent foundation or embankment loading. This approach may also be suitable for mitigating the seismic amplification potential of deep clays sites because thermal consolidation of soft clay layers can be induced without surcharge from the surface. Since pore water pressures will increase in the clay depending on the change in temperature induced by conductive heat flow away from the drain, the excess pore water pressure will dissipate geometrically away from the drain, as well as toward the free drainage boundary of the drain itself. As the magnitude of permanent contraction by heating significantly affects the thermal changes of clay in strength and hydraulic conductivity, it is important for the engineers to have an approach for preliminarily prediction of the magnitude of excess pore water pressures generated by changes in temperature.

This paper is focused on predicting the magnitude of excess pore water pressure generated in clays during undrained heating. An estimate of the magnitude of excess pore water pressure information is needed for the engineering design of thermal drain systems that are used to improve the response of soft clays (Abuel-Naga et al. 2006; Salager et al. 2012). Many researchers have evaluated the undrained heating response of different types of clays under different stress states such as Campanella and Mitchell (1968), Plum and Esrig (1969), Houston et al. (1985), Moritz (1995), Burghignoli et al. (2000), Abuel-Naga et al. (2007), and Uchaipichat and Khalili (2009). These studies found that the magnitude of temperature change, initial void ratio, mean effective stress, stress history quantified using the overconsolidation ratio (OCR), soil structure, and mineralogy of the soil particles play important roles in the magnitude of thermally induced excess pore water pressure generation. Other studies have evaluated the thermal pressurization of saturated rocks (Gabezloo and Sulem 2009; Mohajerani et al. 2012), and in addition to seeing effects from the same variables as in the studies on clays, noted that previous damage or shearing can affect the magnitude of excess pore water pressure generation.

Although Campanella and Mitchell (1968) developed a thermo-poro-mechanical approach assuming thermo-elasticity to estimate the magnitude of change in excess pore water pressure for a

88 given change in temperature using concepts of thermo-elasticity and linear elasticity, some of the

89 parameters in their analysis are not straightforward to define making it difficult to apply in practice. Since

90 this early model was developed, several studies have continued the development of thermo-poro-

91 mechanical theories assuming thermo-elasticity to predict thermal pressurization (McTigue 1986;

92 Aversa and Evangelista 1993; Rice 2006; Ghabezloo and Sulem 2009; Mohajerani et al. 2012) and

93 thermo-elasto-plasticity (Veveakis et al. 2013). An issue that has been identified in these studies is the

94 appropriate definition of material properties that govern the thermal pressurization (Ghabezloo and

95 Sulem 2009). In addition to the topic of interest in this study, predictions of excess pore water pressure

96 and thermal pressurization have been applied to a wide range of topics, including fault rupture in

97 saturated rocks (Wibberley and Shimamoto 2005; Rice 2006; Sulem et al. 2007), shear band formation

98 in landslides (Vardoulakis 2002; Cecinato et al. 2011; Veveakis et al. 2013), and radioactive waste

99 disposal (Mohajerani et al. 2012), which implies that work in this area can have wide-ranging

100 applications.

101 In order to improve the use of the thermo-elastic model of Campanella and Mitchell (1968) in

102 practice, this study proposes an empirical relationship between the key unknown parameters governing

103 thermal excess pore water generation and the geotechnical index properties of soils using data for

104 normally consolidated soils reported in the literature. Further, undrained heating triaxial tests were

105 performed in this study to measure the thermally induced excess pore water pressure in Kaolinite clay

106 under undrained heating conditions in order to validate the proposed relationship. Further, images were

107 taken by using high resolution camera to observe the specimen volume changes during the undrained

108 heating process to fully capture the soil behavior.

2. Theoretical Background

110 Campanella and Mitchell (1968) developed a theoretical approach to estimate the excess pore

111 water pressure generation in a specimen of saturated soil during undrained heating using the concepts

112 of thermo-elasticity and linear elasticity. Specifically, to ensure compatibility of strains during undrained

113 heating, the sum of the changes in volume of the soil constituents due to changes in both temperature

114 and pressure must equal the sum of the volume changes of the total soil mass during changes in

115 temperature ΔT and pore water pressure Δu, as follows:

$$\alpha_w V_w \Delta T + \alpha_s V_w \Delta T - (\Delta V_{st})_{\Delta T} = - m_v V_m \Delta u - m_w V_w \Delta u \qquad (1)$$

116 where α_w is the cubical coefficient of thermal expansion of the pore water, α_s is the cubical coefficient

117 of thermal expansion of the mineral solids, V_w is the initial volume of pore water before heating, V_m is

118 the total volume of the soil mass equal to the sum of V_w and V_s, ΔT is the change in temperature of the

119 soil, Δu is the change in pore water pressure, $(\Delta V_{st})_{\Delta T}$ is the volume change of the soil due to the

120 reorientation and relative movement of the soil particles during heating, m_w is the coefficient of volume

121 compressibility of water and m_v is the coefficient of volume compressibility of soil skeleton. The

122 coefficient of volume compressibility is conventionally defined as the volumetric strain divided by the

123 change in vertical effective stress, but in this study it is defined as the volumetric strain divided by the

124 change in mean stress, as isotropic conditions are assumed. The compressibility of the water is

125 assumed to be negligible compared to the value of compressibility of the soil skeleton. As the porosity

126 of a saturated soil is equal to $n = V_w/V_m$, Equation 1 can be rearranged to estimate the excess pore

127 water pressure generated by a change in temperature during undrained conditions, as follows:

$$\Delta u = \frac{n\,\Delta T\,(\alpha_s - \alpha_w) + \dfrac{(\Delta V_{st})_{\Delta T}}{V_m}}{m_v + n \cdot m_w} = \frac{n\,\Delta T\,(\alpha_s - \alpha_w) + \alpha_{st}\,\Delta T}{m_v + n \cdot m_w} \qquad (2)$$

128 For most soils, the value of m_v is much greater than $n \cdot m_w$ (Campanella and Mitchell 1968), so Equation

129 2 can be simplified as follows:

$$\Delta u = \frac{n\,\Delta T\,(\alpha_s - \alpha_w) + \alpha_{st}\Delta T}{m_v} \qquad (3)$$

3. Estimation of Soil Properties for Pore Water Pressure Prediction

131 Evaluation of Equation 3 indicates that the factors affecting the change in pore water pressure

132 change of saturated soil during undrained heating are the magnitude of the temperature change, the

133 porosity, the difference between the coefficients of thermal expansion for soil grains and water, and the

134 physico-chemical coefficient of the structural volume change. Of these different factors, most can be

135 readily estimated for the soils reported in the literature except for the physico-chemical coefficient of the

136 structural volume change. Specifically, the compressibility of the soil skeleton m_v can be estimated from

137 the compression curve, the values of porosity can be calculated using the initial gravimetric water

138 content and specific gravity, the value of α_s depends on the clay mineral, and α_w is a constant. The

139 values of α_s and α_w used by most researchers such as Campanella and Mitchell (1968), Burghignoli et

140 al. (2000) were equal to 0.000035/°C and 0.00017/°C, respectively. The value of α_s does not vary

141 significantly for the tests on different clay minerals reported in the literature, so the value used by

142 Campanella and Mitchell (1968) can be used to analyze the results from other clays. It is important to

143 clarify that the value of α_w is an order of magnitude greater than α_s, which is one of the primary reasons

144 for the pore water pressure change in saturated clays. However, because the difference between these

145 two parameters is similar for most clays, there must be another parameter that affects the thermal

146 volume change of clays.

147 Regarding the estimation of the value of m_v from the compression curve, Campanella and Mitchell

148 (1968) and Uchaipichat and Khalili (2009) found that a saturated soil will expand along the

149 recompression line during undrained heating. On this basis, the value of m_v can be determined from the

150 isotropic recompression curve $(m_v)_r$ at a given value of mean effective stress, as follows:

$$(m_v)_r = \frac{1}{1 + e_o} \frac{\kappa}{p'} \tag{4}$$

151 where e_0 is the initial void ratio, p' is the mean effective stress, and κ is the slope of the isotropic

152 recompression line equal to $\Delta v / \ln(p'/p'_c)$, where v is the specific volume (v = 1+e) and p'_c is the mean

153 effective preconsolidation stress. As the slope of the isotropic compression line is more commonly

154 reported than the isotropic recompression line in studies on the thermal volume change of normally

155 consolidated soils, the value of κ can be assumed to be related to the slope of the isotropic compression

156 line λ using the ratio $\Lambda = (1-\kappa/\lambda)$. The ratio Λ is typically ranges from 0.7 to 0.9 for low plasticity clays

157 (Schofield and Wroth 1984), and a value of 0.9 was used when the actual value of κ was not reported.

158 Equation 3 can be rewritten in the following form after incorporating the definition of m_v and the ratio Λ:

$$\Delta u \left(\frac{1}{1 + e_o} \right) \frac{(1 - \Lambda)\lambda}{p'} = n \, \Delta T (\alpha_s - \alpha_w) + \alpha_{st} \, \Delta T \tag{5}$$

159 This equation can be solved for the ratio of the pore water pressure to the initial mean effective stress

160 p'_0 before the start of undrained heating, as follows:

$$\frac{\Delta u}{p'_0} = \frac{[n(\alpha_s - \alpha_w) + \alpha_{st}] (1 + e_o)\Delta T}{(1 - \Lambda)\lambda} \tag{6}$$

161 Although this equation contains both the porosity and void ratio, which are directly related [n = e/(1+e)],

162 the value of porosity n is not combined with the initial void ratio because the volume of voids (equal to

163 the volume of water for saturated soil) and the total volume will change by a small amount during

164 undrained heating due to thermal expansion. However, as experimental studies on the thermal excess

165 pore water pressure generation typically do not present the change in total volume of the specimen

166 during undrained heating, it can be assumed that $n = n_0$. This assumption was checked using the

167 experimental total volume change data from this study that will be presented later and similar data from

168 Uchaipichat and Khalili (2009), and the changes in n during undrained heating were found to be small

169 enough that they have a negligible effect on the prediction of pore water pressure generation. The form

170 of Equation (6) confirms that the magnitude of thermally induced excess pore water pressure depends

171 on the initial mean effective stress, a trend that is clear in the data presented by several authors, in

172 particular Uchaipichat and Khalili (2009). The remaining parameter that is not straightforward to

173 estimate for a clay soil is the value of the physico-chemical coefficient α_{st}, which may depend on several

174 parameters. For a normal consolidated clay, it is expected that this parameter depends primarily on the

175 soil mineralogy. Accordingly, the values of α_{st} can be estimated from the Δu data reported for a given

176 ΔT by the different studies in the literature, as follows:

$$\alpha_{st} = \left[\frac{\Delta u}{p'_0} \cdot \frac{(1 - \Lambda) \, \lambda}{1 + e_o} \cdot \frac{1}{\Delta T} \right] - n(\alpha_s - \alpha_w) \tag{7}$$

4. Thermal Soil Response

178 Data from undrained heating tests on saturated soils collected from the literature are investigated

179 in this study. Properties of the soil specimens are shown in Table 1. The Atterberg limits for these clays

180 vary widely (liquid limit LL ranging from 21 to 186 and plasticity index PI ranging from 6 to 109), and the

181 coefficient of compressibility indicates that the soils range from soft (high λ) to stiff (low λ). The liquidity

182 index is greater than 1.0 for many of the soils listed below, indicating that they are wetter than the liquid

183 limit and could have a sensitive response. A summary of the 13 normally-consolidated soil specimens

184 under investigation from these different studies is shown in Table 2, along with the initial mean effective

185 stress at the start of heating of each soil specimen. The soils were all heated by different magnitudes,

186 with the greatest change in temperature being approximately 80 °C.

187 The results of the change in pore water pressure with change in temperature are shown in Figure 1

188 for the different soil specimens listed in Table 2. Due to the difference in the thermal expansion

189 coefficient of water and soil particles, the change in pore water pressure increases with increasing

190 change in temperature. The excess pore water pressure induced by the change in the temperature

191 normalized by the initial effective stress is shown in Figure 2. The spread in the normalized pore water

192 pressure changes is lower than the raw changes in pore water pressure shown in Figure 1. The initial

193 mean effective stress plays an important role, as the stiffness of the soil skeleton is expected to increase

194 with increasing mean effective stress which may affect the pore water pressure generation during

195 heating. The results in Figure 2 imply that greater pore water pressures will be expected deeper in a

196 soil deposit. Further, evaluation of the results in Figure 2 indicates that, for most soils, the thermally

197 induced pore water pressure is greater than half the mean effective stress during a change in

198 temperature of 35 °C. The normalized pore water pressures was consistently less than 1.0, which

199 confirms that thermal failure did not occur in the specimens evaluated in this study.

5. Data Synthesis

201 The values of α_{st} were calculated using Equation 7 for each of the data points in Figure 2. In most

202 cases, the slope for each data set was approximately linear. As there is some scatter in the increase in

203 pore water pressure with temperature for soil specimen SPC2, a best fit slope was obtained for this soil

204 specimen. The trend between the average values of α_{st} and the plasticity index (PI) for the different soil

205 specimens listed in Table 2 is shown in Figure 3. The only study that reported a value of α_{st} was

206 Campanella and Mitchell (1968), who reported a value of 0.00005/°C for SPC1. This value is slightly

207 different from the value of 0.0006/°C calculated for SPC1 using Equation 7 and the normalized changes

208 in pore water pressure for this soil shown in Figure 2. However, they used the results from drained

209 thermal consolidation tests to estimate the value of α_{st}, and also observed a discrepancy when using

210 their value of α_{st} to predict the change in pore water pressure observed during a separate undrained

211 heating test. This may have been due to experimental differences between their drained and undrained

212 heating tests. Further, as noted in Table 1, Campanella and Mitchell (1968) did not report Atterberg

213 limits, so the average PI for a pure Illite reported by Mitchell (1993) was used in plotting Figure 3. The

214 trend in Figure 3 shows the PI has significant effect on the α_{st}. Although there is some scatter, the value

215 of α_{st} decreases nonlinearly with PI. This is especially clear for specimens SPC2 and SPC3 which have

216 very different PI values but were tested under the same initial effective stress and the same testing

217 conditions. Comparison of the values of the α_{st} for the soils that were tested at different initial effective

218 stresses (Houston et al. 1985; Uchaipichat and Khalili 2009; Abuel-Naga et al. 2007) indicates that the

219 initial effective stress does not have a major effect on the value of α_{st}. The small differences for the

220 same soils tested under different effective stresses are due to scatter in the reported experimental

221 changes in pore water pressure with temperature.

222 The effect of the liquidity index LI on the physico-chemical coefficient was studied as well, as this

223 parameter may permit assessment of the role of sensitivity on the thermal volume change. This was

224 performed as several of the clays in the literature had relatively high water contents compared to the

225 liquid limit. The relationship between the physico-chemical coefficient α_{st} and LI is shown in Figure 4.

226 Although no clear trend was observed for the specimens evaluated, it is interesting to note that the

227 specimens with liquidity index values greater than 1.0 had relatively high values of α_{st}

228   As the trends with the plasticity index was found to be the most significant, a best-fit empirical

229 relation between the plasticity index and the physico-chemical coefficient α_{st} was fit to the data as shown

230 in Figure 5. The empirical relationship can be expressed as follows:

$$\alpha_{st} = 1.0 \times 10^{-4} \ e^{-0.014 \ PI} \tag{8}$$

231 Despite the scatter in the data and the low R^2 value, the empirical expression provides a reasonable

232 representation of the trend in the data. Equation 8 may be useful in providing preliminary estimates of

233 the change in pore water pressure during undrained heating of soils.

234 6. Validation of the Model

235 6.1 Materials and Specimen Preparation

236   In order to validate the prediction of the value of α_{st} for a soil in the prediction of the thermally

237 induced pore water pressure, an independent experiment was performed on a saturated, normally

238 consolidated clay specimen. Commercial kaolinite clay from M&M Clays Inc., McIntyre, Georgia was

239 used for the experiment. The geotechnical properties of the clay are summarized in Table 3. As the clay

240 has a liquid limit and plastic index of 47 and 19, respectively, it is classified as CL according to the

241 Unified Soil Classification Scheme (USCS) medium plasticity. The clay has a specific gravity of 2.6.

242   The kaolinite clay layer was prepared by mixing the kaolinite clay powder and deionized water in a

243 vacuum mixer to form a slurry with a water content of 135%. The slurry was then slowly poured into a

244 242 mm-diameter acrylic cylinder with a porous stone and filter on the top and bottom of the specimen.

245 The clay layer was consolidated using a compression frame at a constant rate of 0.04 mm/min for 48

246 hours. After this point, constant vertical stresses of 124, 248, and 352 kPa were applied to the clay layer

247 in 24 hour increments. The preconsolidated clay layer was extruded from the cylinder, and divided into

248 four equal pieces. One of these pieces was then trimmed into a cylindrical specimen having a diameter

249 of 72.4 mm and a height of 147.3 mm. The specimen was then placed into the thermal triaxial cell for

250 testing. The water content and initial void ratio values after consolidation but before application of a

251 change in the temperature are also summarized in Table 3.

252 6.2 Equipment and procedures

253   The test was performed by using a modified triaxial system originally developed by Alsherif and

254 McCartney (2013, 2015). A schematic of the system is shown in Figures 6. The cell is comprised of a

255 Pyrex pressure vessel that has the advantage of having low thermal creep behavior while still remaining

256 transparent after repeated heating and cooling cycles. The temperature within the cell is controlled by

257 circulating heated water from a heated water bath through a stainless steel pipe bent into a "U" shape

258 over the specimen. A solar pump is used to circulate the cell water to ensure that it is uniformly mixed,

259 and a thermocouple is used to monitor the cell temperature changes. A pore water pressure transducer

260 is used to monitor the pore water pressure during undrained heating. The cell fluid temperature was

261 monitored using a thermocouple and temperature recorder having a precision of 0.5 °C. The cell

262 pressure and backpressure were controlled using a pressure panel.

263　　The testing procedure first involved back-pressure saturation of the specimen, which was

264 performed by applying the cell pressure and backpressure in stages until reaching a value of

265 Skempton's pore water pressure parameter B of 0.98 while maintaining a constant seating mean

266 effective stress of 69 kPa. The specimen was then consolidated isotropically to a mean effective stress

267 of 414 kPa, which corresponds to normally consolidated conditions. After this point, the specimen was

268 heated in undrained conditions from 23 to 54 °C in increments of 5 to 10 °C. Each increment was

269 maintained until the pore water pressure stabilized. The rate of heating rate between each increment is

270 approximately 1.3 °C/hr. During the heating process, images of the specimen were taken using a high

271 resolution camera (model D610 from Nikon) to measure changes in volume of the specimen throughout

272 the test.

6.3 Experimental results and analysis

274　　The experimental results from the undrained heating test were illustrated in Figure 7. The thermally

275 induced excess pore water pressure was observed to increase linearly with the change in temperature

276 for the normally consolidated kaolinite clay. The physico-chemical coefficient was estimated using

277 Equation 8 to be α_{st} = 7.7×10^{-5} 1/°C, which was then used to predict the pore water pressure as a

278 function of temperature using Equation 3. The predicted thermally induced pore water pressures are

279 also shown in Figure 7, and good correspondence between the experimental and predicted pore water

280 pressures for the normally consolidated kaolinite clay are observed. As a check, the physico-chemical

281 coefficient was also calculated using Equation 7 with the experimentally measured pore water pressure

282 values to be α_{st} = 9.1×10^{-5} 1/°C, which is a reasonable match with the empirically-estimated value. This

283 confirms that the proposed empirical equation can be used as part of preliminary predictions of the

284 generation of pore water pressure during undrained heating, and that the magnitude of α_{st} can be

285 determined by basic properties of soils and knowledge of the current stress condition without having to

286 perform complex experiments.

287   Images were taken during the undrained heating test to measure the effect of the temperature

288 change on the specimen volume. The specific volume v plotted against the mean effective stress

289 (calculated as the initial effective stress minus the thermally induced pore water pressure) at

290 temperatures of 24, 40.5, and 53 °C is shown in Figure 8. The specific volume increased with

291 temperature along the elastic recompression curve (κ = -0.0136). The isotropic compression curve with

292 an unloading cycle for the kaolinite clay (measured from an isotropic consolidation test performed on a

293 separate specimen of the clay under the same initial conditions) is also shown in Figure 8. Similar to

294 observations of Uchaipichat and Khalili (2009), the value of κ from the recompression curve is similar

295 to that measured from the thermal volume changes during the undrained heating test. This confirms the

296 choice of κ in the definition of the physico-chemical coefficient of structural volume change in

297 Equation 4.

7. Role of Stress History in Pore Water Pressure Prediction

299   Although the model for the physico-chemical coefficient in Equation 8 was developed using tests

300 on soils under normally consolidated conditions, it may also be possible to apply use this parameter to

301 predict the thermally induced pore water pressures in overconsolidated soils. When unloading a

302 normally consolidated soil along the recompression curve, the void ratio will increase and the value of

303 p' will decrease. These two variables play a key role in the predicting the thermally induced pore water

304 pressure using Equation 6. Relatively few studies have investigated the thermally induced pore water

305 pressure in overconsolidated clays. One such study is Abuel-Naga et al. (2007), who evaluated the

306 behavior of overconsolidated specimens in addition to investigating the effects of temperature on the

307 pore water pressure in normally consolidated Bangkok clay specimens. Their experimental results were

308 compared with the prediction from Equation 6 using the same value of α_{st} as that defined for the normally

309 consolidated specimens, but with different values of initial void ratio, porosity, and initial effective stress.

310 The comparison is shown in Figure 9. A good match was obtained for the specimens with increasing

311 OCR values, which confirms the flexibility of the model in considering different stress states in the

312 prediction of the thermally induced excess pore water pressure. Additional research is needed to

313 evaluate whether Equation 6 could be used to evaluate thermal pressurization in saturated rocks, a

314 topic that has been studied by Ghabezloo and Sulem (2009) and Mohajerani et al. (2012). An issue

315 with that may be encountered is that the plasticity index is typically not measured for rock specimens.

8. Conclusion

317   A prediction model for the thermally induced pore water pressure was proposed and experimentally

318 validated in this study. Normalized pore water pressures measured during changes in temperature

319 during undrained heating tests on soil specimens reported in the literature were used to calculate the

320 physico-chemical coefficient. Normalization of the pore water pressures helped remove the effects of

321 the initial effective stress from the analysis, and specimens of the same soil tested under different initial

322 mean effective stresses had similar physico-chemical coefficients of structural volume change.

323 Relationships between the calculated values of the physico-chemical coefficient and the plasticity index

324 and liquidity index were investigated. Although a nonlinear decreasing trend was observed with the

325 plasticity index, no trend was observed with the liquidity index. A prediction model was proposed based

326 on an empirical relationship between the physico-chemical coefficient of structural volume change and

327 plasticity index. The pore water pressure values predicted by this model for kaolinite clay were matched

328 well with those measured in an independent undrained heating test. This confirms that this simple,

329 empirical approach to define the physico-chemical coefficient in the thermo-elastic model is effective in

330 making preliminary estimates of the thermally induced pore water pressures expected in saturated soils

331 used in thermal soil improvement or in thermally active geotechnical engineering systems. The thermal

332 expansion of the specimen calculated using image analysis was found to match well with the slope of

333 the recompression curve, confirming the assumption of the magnitude of the coefficient of volume

334 compressibility used in the analysis. Although only limited data is available in the literature for

335 overconsolidated clays, the validated model was found to also provide a good fit to the thermally

336 induced pore water pressure in saturated, overconsolidated clays.

References

Abuel-Naga, H.M., Bergado, D.T., Suttisak, S. "Innovative thermal technique for enhancing the performance of prefabricated vertical drain system." Geotextiles and Geomembranes. 24, (2006), 359–370.

Abuel-Naga, H.M., Bergado, D.T., Bouazza, A. "Thermally induced volume change and excess pore water pressure of soft Bangkok clay." Engineering Geology. 89, (2007) 144-154.

Alsherif, N.A., McCartney, J.S. "Triaxial cell for nonisothermal shear strength of compacted silt under high suction magnitudes." Proceedings of the 1st Pan-American Conference on Unsaturated Soils. Feb. 20-22. Cartagena de Indias. Taylor and Francis Group, London. (2013). 147-152.

Alsherif, N.A., McCartney, J.S. "Nonisothermal behavior of compacted silt at low degrees of saturation." Géotechnique. (2015). DOI: 10.1680/geot./14-P-049.

Aversa, S., Evangelista, A. "Thermal expansion of Neapolitan yellow tuff." Rock Mechanics and Rock Engineering. 26(4), (1993) 281-306.

Baldi, G., Hueckel, T., Pellegrini, R. "Thermal volume changes of the mineral-water system in low-porosity clay soils." Canadian Geotechnical Journal. 25(4), (1988), 807-825.

Burghignoli, A., Desideri, A., Miliziano, S. "A laboratory study on the thermomechanical behavior of clayey soils." Canadian Geotechnical Journal. 37(4), (2000), 764-780.

Campanella, R.G., Mitchell, J.K. "Influence of temperature variations on soil behavior." Journal of the Soil Mechanics and Foundation Division, 94(SM3), (1968), 709-734.

Cecinato, F., Zervos, A., Veveakis, E. "A thermo-mechanical model for the catastrophic collapse of large landslides." International Journal of Numerical and Analytical Methods in Geomechanics. 35(14), (2011), 1507-1535.

Ghabezloo S., Sulem J. "Stress dependent thermal pressurization of a fluid-saturated rock." Rock Mechanics and Rock Engineering Journal. 42, (2009), 1-24.

Houston, S.L., Houston, W.N., Williams, N.D. "Thermo-mechanical behavior of seafloor sediments." Journal of Geotechnical Engineering. 111(12), (1985), 1249-1263.

Mitchell, J.K. Fundamentals of Soil Behavior. 2nd Edition. Wiley, New York. (1993).

Mahajerani, M., Delage, P., Sulem, J., Monfared, M., Tang, A.M., Gatmiri, B. "A laboratory investigation of thermally induced pore pressures in the Callovo-Oxfordian Claystone." International Journal of Rock Mechanics and Mining Sciences. 52, (2012), 112-121. doi:10.1016/j.ijrmms.2012.02.012.

371 McTigue, D.F. "Thermoelastic response of fluid-saturated porous rock." Journal of Geophysical

372 Research. 91(B9), (1986), 9533–9542.

373 91(B9):9533–9542.Moritz, L. Geotechnical Properties of Clay at Elevated Temperatures. Report 47,

374 Swedish Geotechnical Institute, Linköping, Sweden. (1995).

375 Plum, R.L., Esrig, M.I. "Some temperature effects on soil compressibility and pore water pressure."

376 Highway Research Board, Washington, DC. Report 103. (1969), 231–242.

377 Rice, J.R. "Heating and weakening of faults during earthquake slip." Journal of Geophysics Research.

378 111, B05311, doi:10.1029/2005JB004006. (2006).

379 Salager, S., Laloui, L., Nuth, M. "Efficiency of thermal vertical drains for the consolidation of soils."

380 Proceedings of 2nd Int. Conf. on Transportation Geotechnics, Hokkaido, Japan. (2012). 1-10.

381 Schofield, A., Wroth, P. Critical State Soil Mechanics. Cambridge University. (1973).

382 Sulem, J., Lazar, P., Vardoulakis, I. "Thermo-poro-mechanical properties of clayey gouge and

383 application to rapid fault shearing." International Journal of Numerical and Analytical Methods in

384 Geomechnics. 31(3), (2007), 523-540.

385 Uchaipichat, A. Khalili, N. "Experimental investigation of thermo-hydro-mechanical behaviour of an

386 unsaturated silt." Géotechnique. 59(4), (2009), 339–353.

387 Vardoulakis, I. "Dynamic thermo-poro-mechanical analysis of catastrophic landslides." Géotechnique,

388 52, (2002), 157-171.

389 Veveakis, E., Stefanou, I., Sulem, J. "Failure in shear bands for granular materials: Thermo-hydro-

390 chemo-mechanical effects." Géotechnique Letters. 3(2), (2013), 31-36.

391 Wibberley, C., T. Shimamoto, T. "Earthquake slip weakening and asperities explained by thermal

392 pressurization." Nature, 426(4), (2005), 689-692.

393 **Table and Figure captions**

394 **Table 1.** Properties of the soil specimens reported in the literature.

395 **Table 2.** The numbers designations for the soil specimens evaluated in the study.

396 **Table 3.** Properties of the Kaolinite clay.

397 **Figure 1.** Effect of temperature change on the change in pore water pressure for all soil specimens.

398 **Figure 2.** Effect of temperature change on the change in pore water pressure normalized by the initial

399   effective stress for all soils specimens.

400 **Figure 3.** Effect of temperature change on the change in pore water pressure normalized by the initial

401   effective stress for all soils specimens.

402 **Figure 4.** Physico-chemical coefficient as a function of liquidity index for different clays from the
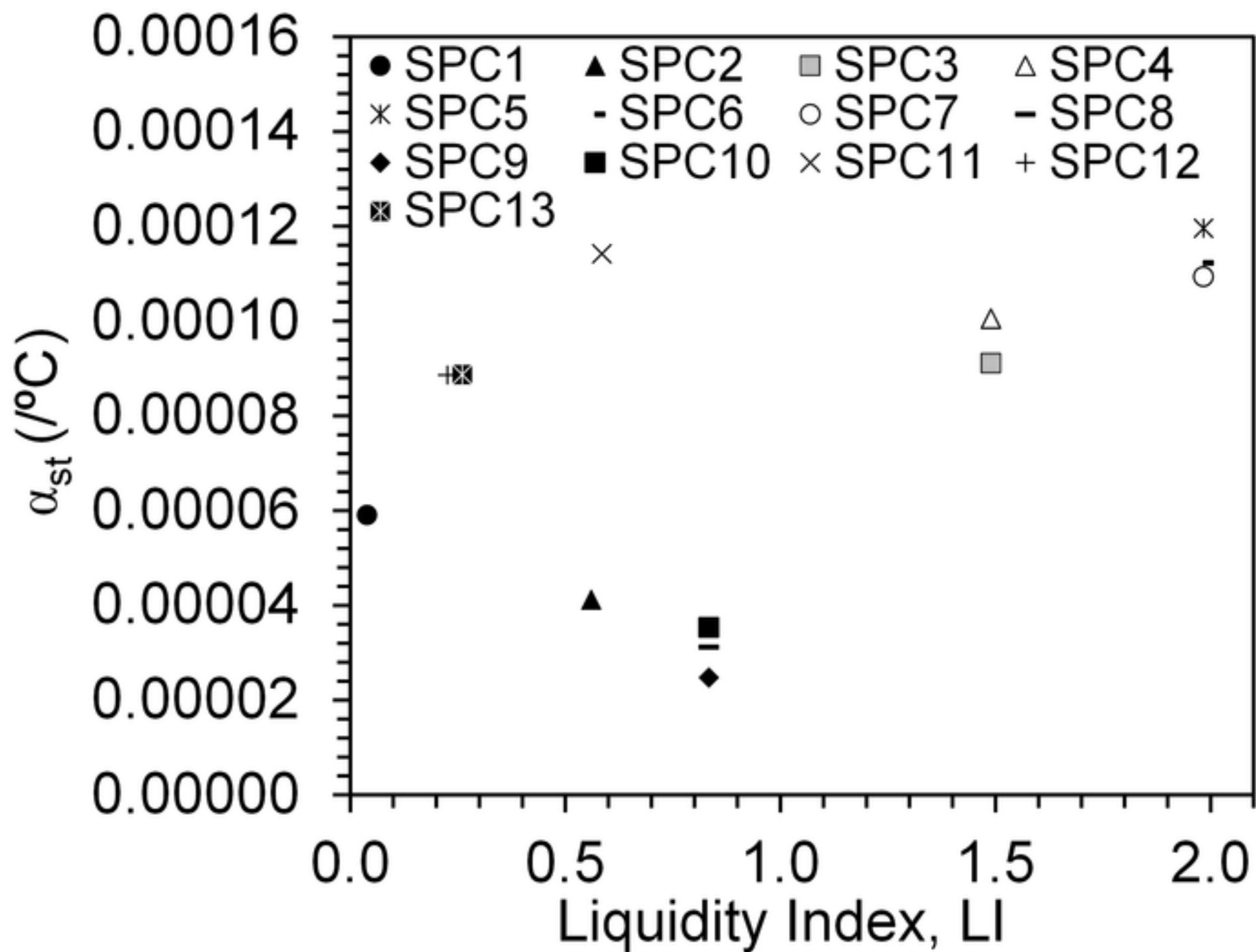
403   literature.

404 **Figure 5.** Physico-chemical coefficient as a function of plasticity index for different clays from the
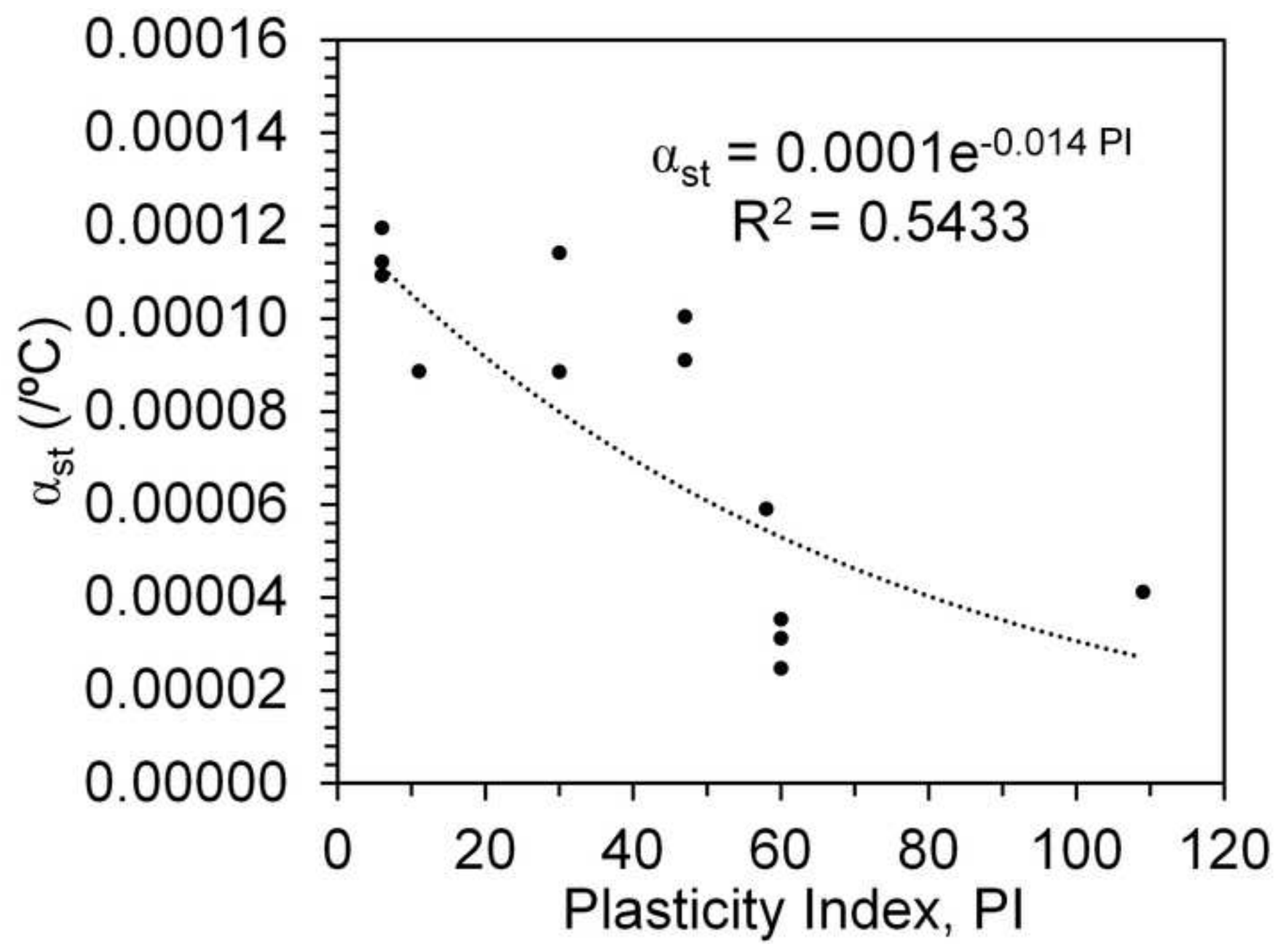
405   literature.

406 **Figure 6.** Thermal triaxial cell schematic.
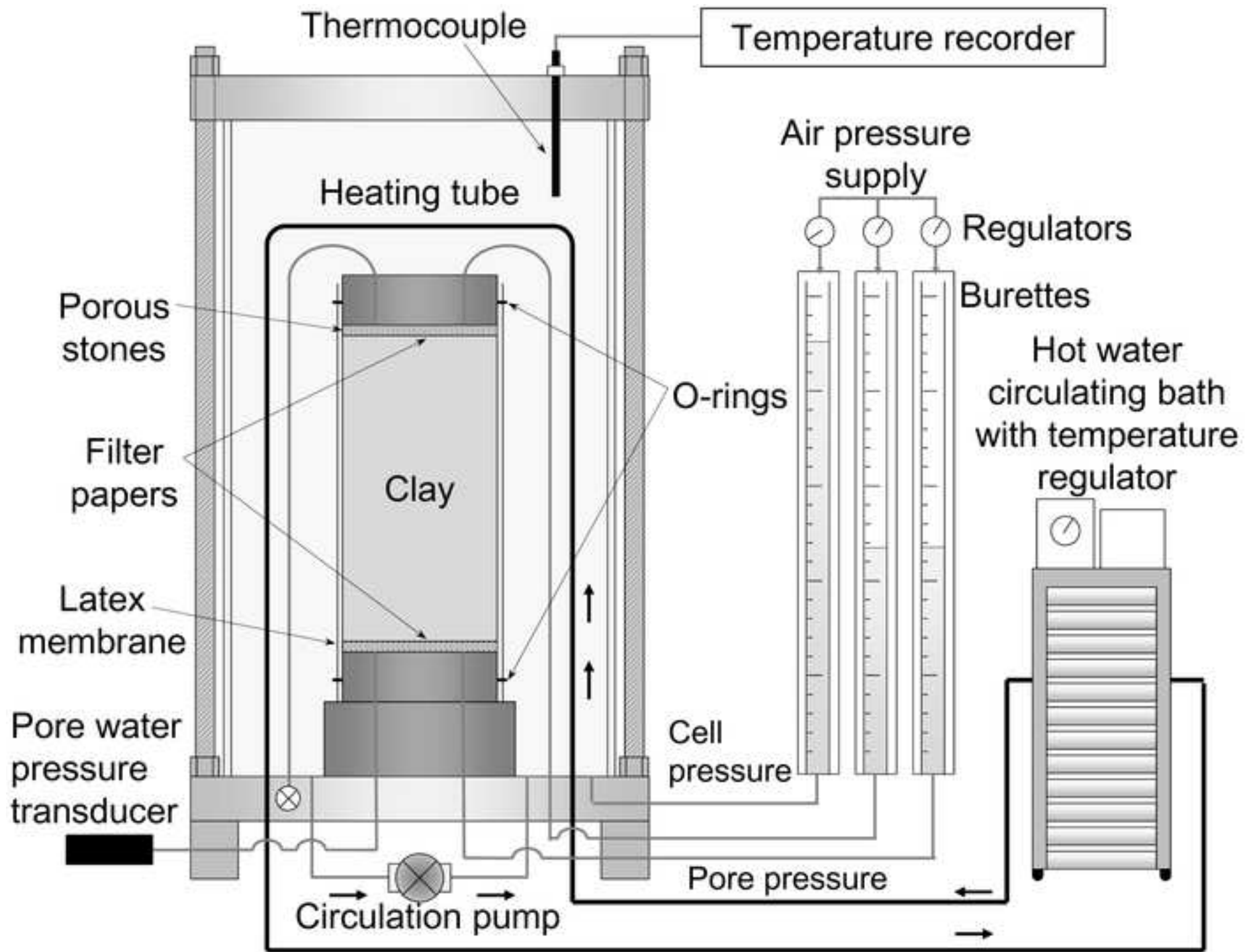
407 **Figure 7.** Effect of temperature change on the change in pore water pressure for kaolinite clay along

408   with the predicted trend using the estimated value of the physico-chemical coefficient of

409   structural volume change.

410 **Figure 8.** Specific volume against isotropic effective stress during heating.

411 **Figure 9.** Impact of temperature change on the change in pore water pressure in Bangkok clay

412   specimens having different OCRS along with predicted pore water pressure trends.

413

414 **Table 1.** Properties of the soil specimens reported in the literature.

Reference	Soil Type	e_0	w (%)	LL	PI	λ	Main Minerals
Campanella and Mitchell (1968)	Remolded Illite Clay	0.90	34	94[*]	62[*]	0.39	Illite
Plum and Esrig (1969)	Newfield Clay	0.50	18	25	11	0.09	Chlorite, Mica
Houston et al. (1985)	Illite Clay	2.90	111	88	47	0.43	Quartz, Illite
Houston et al. (1985)	Pacific Smectite Clay	3.70	138	186	109	0.52	Smectite, Illite
Abuel-Naga et al. (2007)	Bangkok Clay	2.50	93	103	60	0.46	Smectite, Kaolinite, and Mica
Uchaipichat and Khalili (2009)	Bourke Silt	0.70	26	21	6	0.09	Not reported
Burghignoli et al. (2000)	Todi Clay	0.89	40	52	30	0.1	Montmorillonite, Illite, Kaolinite, Calcite, Quartz
Burghignoli et al. (2000)	Fiumicino Clay	0.81	30	55	32	0.09	Not reported

415 *Note: Values not reported in the original study, the values shown here are for a typical pure Illite clay

416

417 **Table 2.** The numbers designations for the soil specimens evaluated in the study.

Specimen Number	Soil Type	Reference	p' (kPa)
SPC1	Remolded Illite Clay	Campanella and Mitchell (1968)	196
SPC2	Pacific Specitite Clay	Houston et al. (1985)	98
SPC3	Illite Clay	Houston et al. (1985)	98
SPC4	Illite Clay	Houston et al. (1985)	29
SPC5	Bourke Silt	Uchaipichat and Khalili (2009)	50
SPC6	Bourke Silt	Uchaipichat and Khalili (2009)	100
SPC7	Bourke Silt	Uchaipichat and Khalili (2009)	150
SPC8	Bangkok Clay	Abuel-Naga et al. (2007)	200
SPC9	Bangkok Clay	Abuel-Naga et al. (2007)	300
SPC10	Bangkok Clay	Abuel-Naga et al. (2007)	400
SPC11	Todi Clay	Burghignoli et al. (2000)	196
SPC12	Fiumicino Clay	Burghignoli et al. (2000)	147
SPC13	Newfield Clay	Burghignoli et al. (2000)	275

418

419 **Table 3.** Properties and initial conditions of the Kaolinite clay specimen evaluated in this study.

LL	47
PL	28
PI	19
w_0 (%)	31
G_s	2.6
e_0	0.81
n	0.45

420

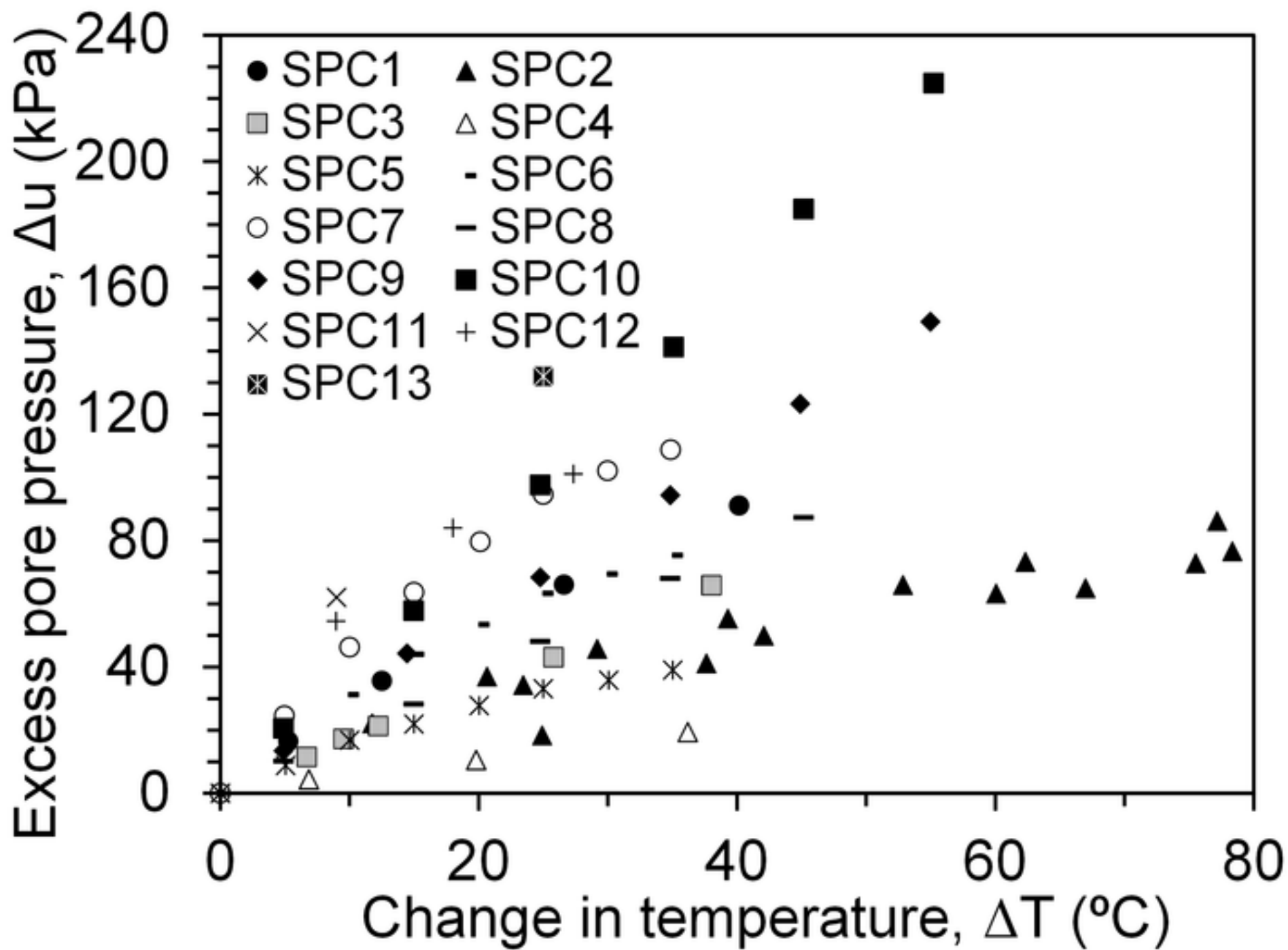Figure 1. Effect of temperature change on the change in pore water pressure for all soil specimens.

Figure 2. Effect of temperature change on the change in pore water pressure normalized by the initial effective stress for all soils specimens.
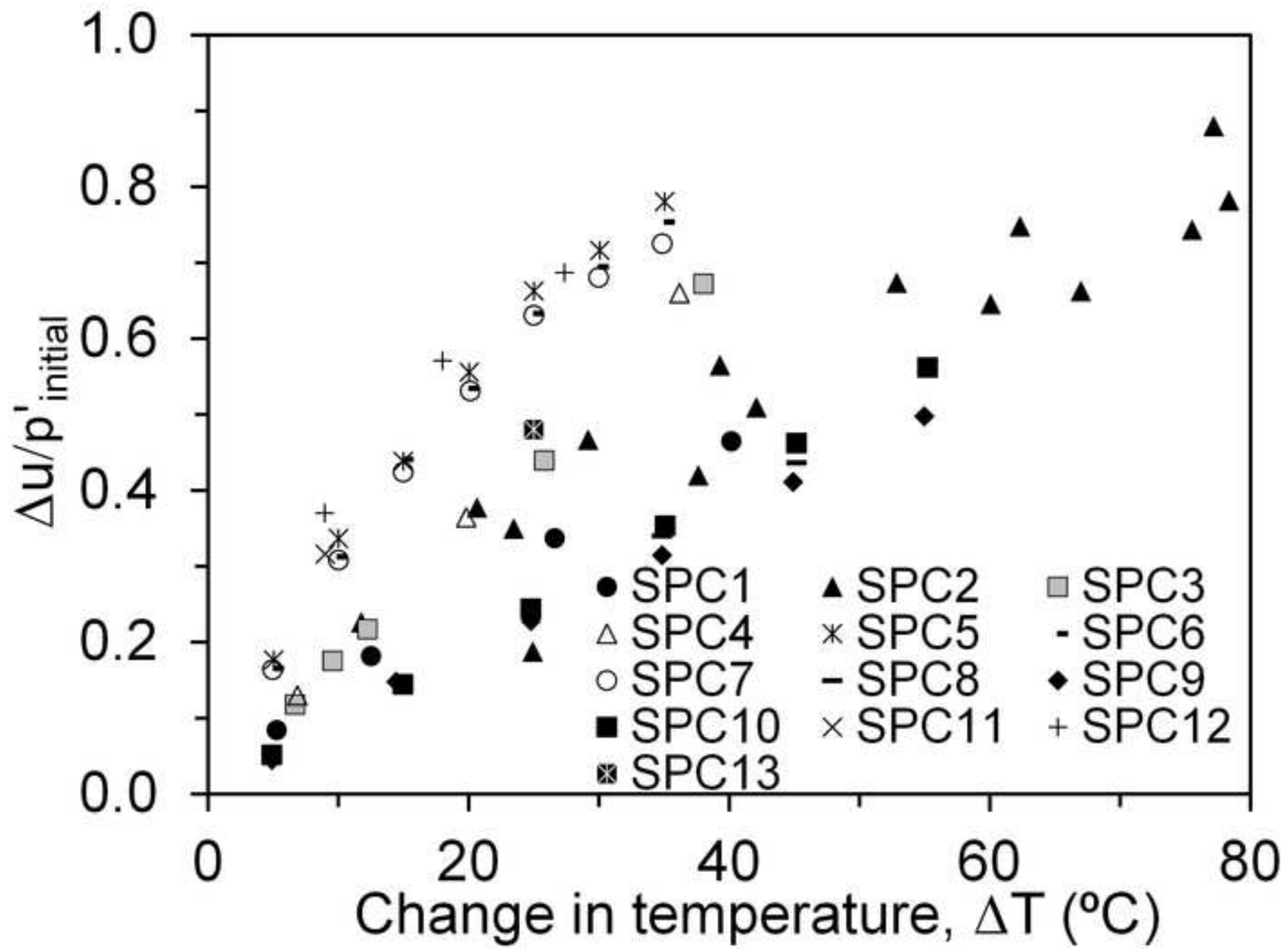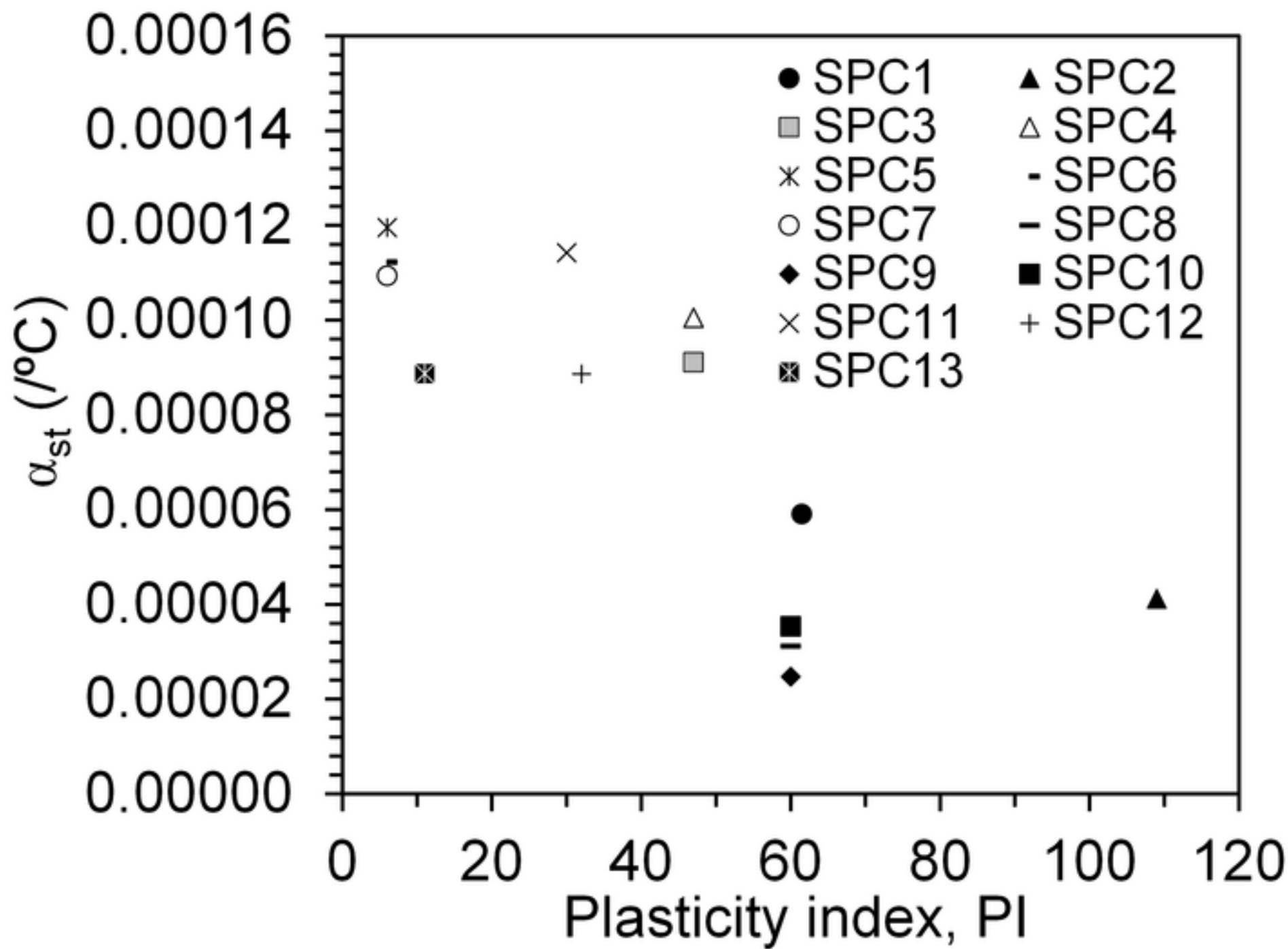
Figure 3. Effect of temperature change on the change in pore water pressure normalized by the initial effective stress for all soils specimens.

The figure shows a scatter plot with the fitted relationship:

$$\alpha_{st} = 0.0001e^{-0.014\,PI}$$

$$R^2 = 0.5433$$

with the y-axis labeled $\alpha_{st}\ (/^{\circ}C)$ and the x-axis labeled Plasticity Index, PI.

Figure 6. Thermal triaxial cell schematic.

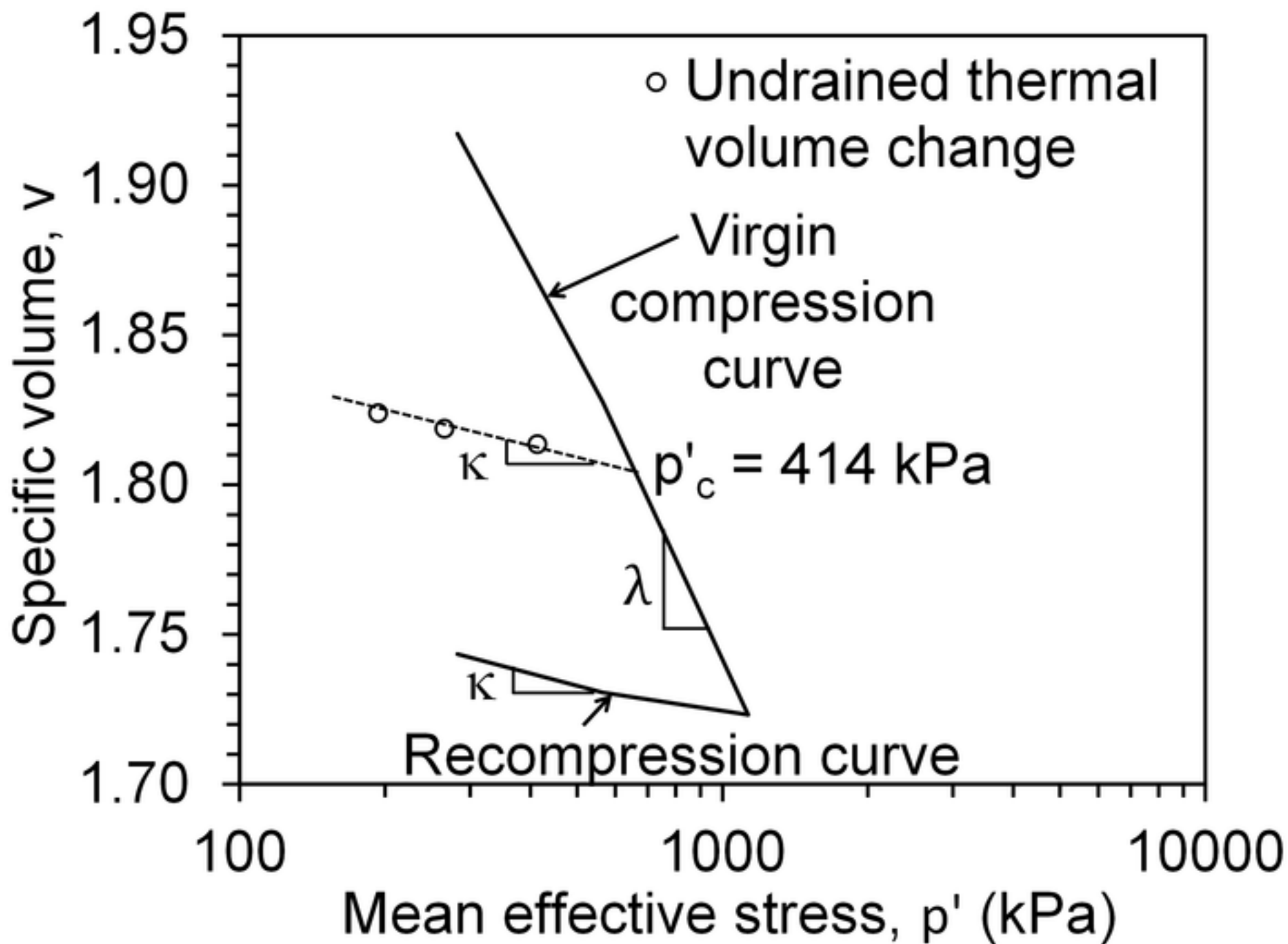Figure 8. Specific volume against isotropic effective stress during heating.

Figure 9. Impact of temperature change on the change in pore water pressure in Bangkok clay specimens having different OCRS along with predicted pore water pressure trends.